

# Error Detection, Error Recovery and Safe Navigation for Autonomous Mobile Systems

D. Bank

Research Institute for Applied Knowledge Processing (FAW)  
Helmholtzstr. 16  
D-89081 Ulm, Germany  
bank@faw.uni-ulm.de

## Abstract

*This paper presents an approach to safe navigation of autonomous mobile systems within partially known or unknown dynamic environments. In this context, faulty, maladjusted and otherwise influenced sensors must be recognized (error detection), and adequate measures for failure correction (error recovery) must be taken. Furthermore, reliable recognition of objects which are difficult to detect must be achieved.*

*As a general basis for monitoring the state of environmental sensors, a so called "error detection model" was created, which consists of sub-models for data from laser range finders and ultrasonic sensors. With the aid of the created models, different kinds of redundancy can be utilized and consistency and plausibility checks can be carried out. The error detection model serves for failure recognition based on environment modeling. It is supplemented by active sensor tests using hypotheses for expected sensor readings.*

**Keywords:** *autonomous mobile robots, robust sensing, error detection, error recovery, sensor data fusion, sensor fault detection*

## 1 Introduction

Considering the navigation of autonomous mobile systems in only partially known or unknown dynamic environments, the complete contactless sensory coverage of the workspace represents a fundamental difficulty. To overcome this problem, several sensor systems (having different positive and negative properties) are used in combination. However, during operation of autonomous systems in real environments (e. g. homes, offices, industrial plants, railway stations,

exhibition halls) many objects appear which cannot be reliably detected by any of the employed sensor systems (e. g. mirrors, panes, shiny metal surfaces, table edges, fences, clotheslines, stairheads, show-cases, shelves and racks). In many cases tactile sensors serve as safety deactivation, whereas they often also cannot cover the whole potential collision range.

Failures or interferences of individual sensor systems represent another challenge. For instance, it frequently occurs that individual sensors are covered or otherwise impaired (e. g. by unfavorable light conditions). In such cases it is important to recognize the condition of the sensor and to initiate suitable remedies.

Our objective is the collision-free navigation of autonomous mobile systems within the above mentioned environments. In this context, faulty, maladjusted and otherwise influenced sensors must be recognized, and adequate measures for failure correction must be taken. Furthermore, reliable recognition of objects which are difficult to detect must be achieved with contactless sensors.

As a general basis for monitoring the state of environmental sensors, a so called error detection model was created, which consists of sub-models for laser range finders and for ultrasonic sensors. The models for laser data are based on line extraction for polygonal environments; the models for ultrasonic distance measurements depend on direct and cross echo evaluation. With the aid of the created models, physical, analytical, spatial and temporal redundancy can be utilized and consistency and plausibility checks can be carried out. The error detection model serves for failure recognition based on environment modeling. It is supplemented by active sensor tests using hypotheses for expected sensor readings. In order to promote specific error recovery, failure classification can be per-

formed.

Measures for failure correction comprise sensor employment planning as well as a context dependent (i. e. situation and environment dependent) sensor data fusion. Other important aspects are the use of redundant hardware and alternative control strategies as well as virtual sensors and automatic sensor calibration.

The described models were tailored for an intelligent wheelchair (MAid) developed at FAW Ulm as well as for an experimental robot XR4000 from Nomadic Technologies. MAid (mobility aid for elderly and disabled people) was designed to autonomously or semi-autonomously transport people through private and public environments [6]. The experimental robot XR4000 at FAW serves for simulating an automatically guided hospital bed (AutoBed) [1]. For these applications the proposed safety features are particularly important.

Within this paper we focus on the developed error detection model, by describing the overall model and the sub-models for data from laser range finders and ultrasonic sensors in detail. We describe the models for the sensor arrangement on a circular robot and we demonstrate their behavior in a typical office environment.

In respect of related work concerning fault detection of ultrasonic sensors on mobile robots we refer to [7]. In this research fault detection is based on a grid representation of the environment. The grid map is constructed using a probabilistic sensor model, similar to [3]. With the use of an occupancy grid it is possible to compare sensor readings made by different sensors, at different points in time and space and from various angles of view. In contrast to this research our approach does not inherently depend on spatial or temporal redundancy, i. e. it does not require a movement of the robot in space in order to allow sensors to make redundant statements.

Before presenting our approaches, we will in section 2 shortly describe a new self-developed ultrasonic sensing system, which serves as the basis for the developed algorithms. Deriving an environment model from the laser range finder data is explained in section 3, and deriving a simulation model for the ultrasonic sensing system will be described in section 4. Sensor evaluation by comparison between simulated and real ultrasonic sensor readings is addressed in section 5, and sensor evaluation by calculation of intersections for the real ultrasonic sensor readings will be described in section 6. How to perform a reliable and robust overall sensor assessment is explained in section 7 and

a conclusion will be presented in Section 8.

## 2 Description of the Sensing Systems

Within this paper we explain our algorithms based on a sensor arrangement for the experimental robot XR4000, which is used for modeling an automatically guided hospital bed. The XR4000 at FAW has been additionally equipped with a new self-developed ultrasonic sensing system and with 2 antipodal Laser Ranging Systems from SICK Electro-Optics.

The new ultrasonic sensing system consists of a ring of 24 sensors, spaced with an angular displacement of  $15^\circ$  and mounted on top of the robot. In contrast to other research work ([2], [3], [4], [7]), which widely used ultrasonic range finders from Polaroid Corporation with a detection cone of  $30^\circ$ , we employ wide-angled sensors from Robert Bosch GmbH with a detection range of  $120^\circ$  in one axis and a detection range of  $60^\circ$  in the other axis. The latter sensors were primarily manufactured for automotive use, e. g. for parking pilots [8].

Wide-angled ultrasonic transducers can on the one hand detect objects within a broader range, but on the other hand make it more difficult to estimate within this broader range the actual location of the object causing the echo. In order to gain a substantial advantage of the broader detection range, we propose to exploit the overlapping of the detection cones from neighbor sensors when they are placed close enough to each other and the angular displacement is not larger than the detection range.

In the case of the new sonar sensing system for the XR4000 we arranged the 24 Bosch sensors exactly above the upper ring of 24 Polaroid sensors which this robot is originally equipped with. This facilitates comparison of the two sonar sensing systems. Furthermore we orientate the sensors with the  $60^\circ$  detection range to a horizontal alignment and we use the  $120^\circ$  range for vertical object detection. With this kind of sensor arrangement we obtain beam-width overlapping up to the third neighbor sensor on each side. We could also orientate the sensors with the  $120^\circ$  detection range to a horizontal alignment and would then obtain beam-width overlapping with even more neighbor sensors.

The 2 laser range finders are also mounted on top of the robot in order to just scan above the sonar ring, which facilitates comparison between sonar readings and laser readings.

### 3 Deriving an Environment Model from Laser Range Finder Data

As a basis to systematically compare sonar readings with laser readings, a polygonal model of the environment was extracted from the laser range finder data. Figure 1 displays the distance readings measured with the two laser scanners. The scanners are usually configured to carry out a  $360^\circ$ -scan with a resolution of  $0.5^\circ$ , consequently delivering up to 722 sample points for a complete scan around the robot. The first laser scanner was orientated in positive y-direction and the second laser scanner in negative y-direction. Hence the distance readings depicted as crosses result from the first scanner and the distance readings depicted as circles result from the second scanner. We might observe that the resolution of the distance readings of scanner 1 is lower than that of scanner 2, since scanner 1 is a PLS scanner with 50 mm distance resolution and scanner 2 is a LMS scanner with 10 mm distance resolution.

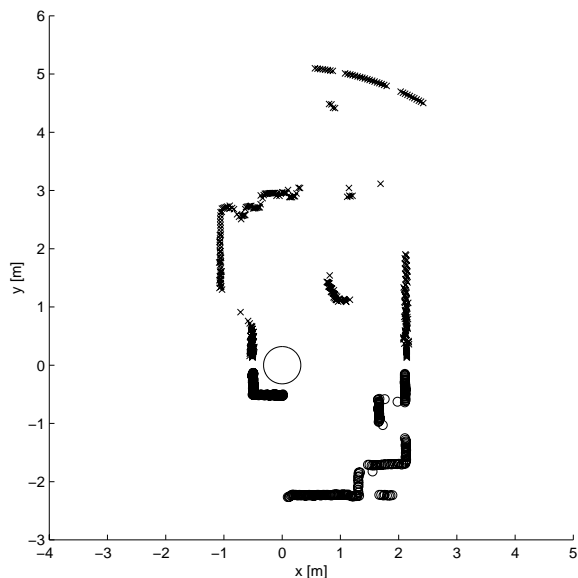


Figure 1: Distance readings measured with 2 antipodal laser range finders

To create a polygonal model which fits to the data of both laser range finders we proceed in the following way: First we combine the samples from both scanners to a single list of distance readings. Then we draw a line through the first and the last data point within this list, i. e. the first sample of scanner 1

at  $0^\circ$  and the last sample of scanner 2 at  $360^\circ$ . Subsequently we calculate the distance of all intermediate data points to this line and determine the data point with the largest distance to the line. Now we divide the list of distance readings at this point and create a reduced list, which only contains the samples up to the dividing point. Thereafter we fit a regression line through the data points of the reduced list and calculate the standard deviation. If the standard deviation is lower than a predefined threshold, the obtained regression line will be the first element of the polygonal model to be created. If the standard deviation is higher than the threshold, we draw a new line through the first and the last data point within the reduced list. Then we again calculate the distance of all intermediate data points to this line and determine the data point with the largest distance to the line, which will be the next dividing point for creating a further reduced list of distance readings. Now we fit a regression line through the data points of the further reduced list and again calculate the standard deviation. We continue these steps recursively until a regression line with a standard deviation lower than the predefined threshold was found. The final dividing point will then be the start point for determining the next element of the polygonal model. For this purpose we create a list which contains the distance readings from the final dividing point up to the last data point within the original list at  $360^\circ$ . Based on this list we proceed in the same manner as described above. We continue in this way until regression lines have been fitted to all data points from the original list of distance readings. Now we still have to close the polygonal model between the last and the first data point. We therefore merge the data points belonging to the last regression line and those appertaining to the first regression line to a new list. Then we fit a new regression line through the data points of this list and check whether the standard deviation is still lower than the predefined threshold. If this is the case, we replace the former two regression lines by the new one. If it is not the case, we divide the new list of data points according to the described method in order to create two or more regression lines, which then replace the former two regression lines. A suitable threshold for the standard deviation was heuristically ascertained to  $\sigma = 0.022m$  (variance  $\sigma^2 = 0.0005m^2$ ). For related literature see [5].

After having determined all elements of the polygonal model, the intersections between consecutive lines can be calculated. Furthermore it is desired to distinguish between line segments which describe existent

features of the environment and pseudo line segments which arise from the visibility angle of the laser range finders. Using Hesse's normal form of the equation of a line with the distance  $p$  from the point of origin in the coordinate system and the angle  $\alpha$  between the normal of the line and the x-axis, the existence of a pseudo line segment is assumed if  $p \leq 0.2m$ . This value was also found heuristically.

Figure 2 shows the obtained polygonal model of the environment, including all line segments, pseudo line segments and their intersections, which are illustrated as solid lines, dashed lines and points respectively.

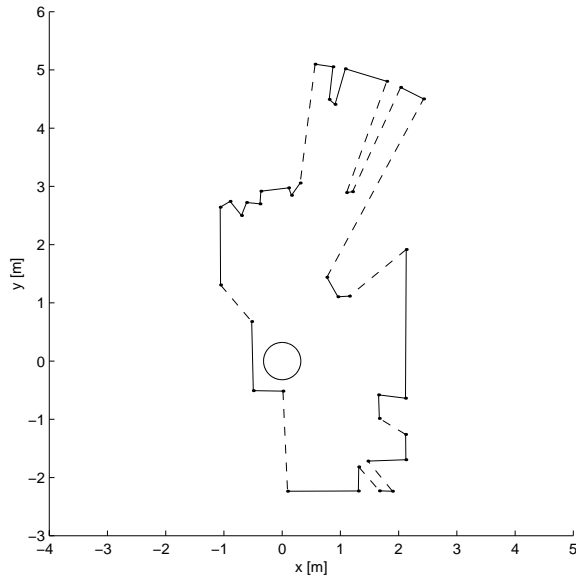


Figure 2: Polygonal model of the environment

#### 4 Deriving a Simulation Model for the Ultrasonic Sensing System

The environment model which we created from laser range finder data now serves as a basis to derive a simulation model for the ultrasonic sensing system.

First we define the detection ranges for the direct and cross echos. We speak about direct echos when the transmitting sensor also receives the signal, and we speak about cross echos when one of the neighbor sensors receives it. With the chosen sensor orientation, the horizontal detection range for direct echos is  $60^\circ$  and for cross echos approximately  $45^\circ$ ,  $30^\circ$  or  $15^\circ$ , depending whether the first, second or third neighbor sensor is involved, since the angular displacement of the sensors is  $15^\circ$ . Consequently we obtain 24 direct echo paths and 144 ( $= 6 * 24$ ) cross echo paths. Direct

echos paths can be depicted as circular arcs with  $60^\circ$  and cross echos paths as elliptic arcs with about  $45^\circ$ ,  $30^\circ$  or  $15^\circ$ .

Regarding the environment model we distinguish between planes, corners and edges according to [4]:

1. A plane is represented by a line in the two-dimensional environment model. Lines are represented in Hesse's normal form.
2. A corner is a concave dihedral, and produces specular returns. Corners are represented as points in the two-dimensional model.
3. An edge is a convex dihedral, and produces diffuse reflections. Like a corner, an edge is represented by a point in the two-dimensional model.

Experiments with the employed ultrasonic sensors have shown that detectable echos predominantly arise from planes and corners, since edges produce diffuse reflections. For this reason, possible reflections from edges are neglected, and only returns from planes and corners are considered in the simulation model for the ultrasonic sensing system.

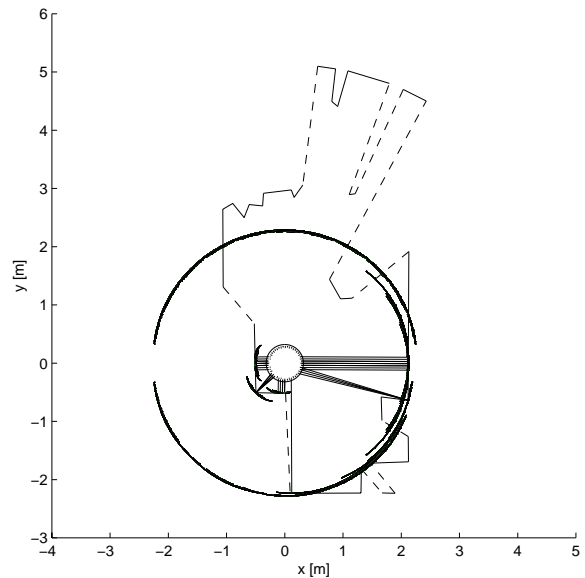


Figure 3: Simulation model of the ultrasonic sensing system

To create the ultrasonic simulation model we consider all planes and corners of the environment model and verify whether they could cause detectable echos, i. e. reflections which fall within the detection range for direct or cross echos of any sensor. Here we have to consider that planes (lines in the two-

dimensional model) or corners (points in the two-dimensional model) can be occluded. A line is occluded if a perpendicular drawn from the line to the sensor intersects another element of the polygonal model; a point is occluded if a line drawn from the point to the sensor intersects another element of the polygonal model. Finally we respectively assign the shortest detectable distance to each direct and cross echo path. Figure 3 shows the circular and elliptic arcs for all direct and cross echo paths. Echo paths with no detectable echo within the operating range of the sensors are represented by arcs corresponding to the maximum distance detection range ( $d_{max} \approx 2m$ ).

## 5 Sensor Evaluation by Comparison between simulated and real Ultrasonic Sensor Readings

In section 4 we described how the shortest detectable distance was assigned to each direct and cross echo path in order to create the ultrasonic simulation model. Within this section we compare the actual distance readings obtained from the sensing system to the results obtained with the simulation model. Figure 4 displays the circular and elliptic arcs for the real distance readings.

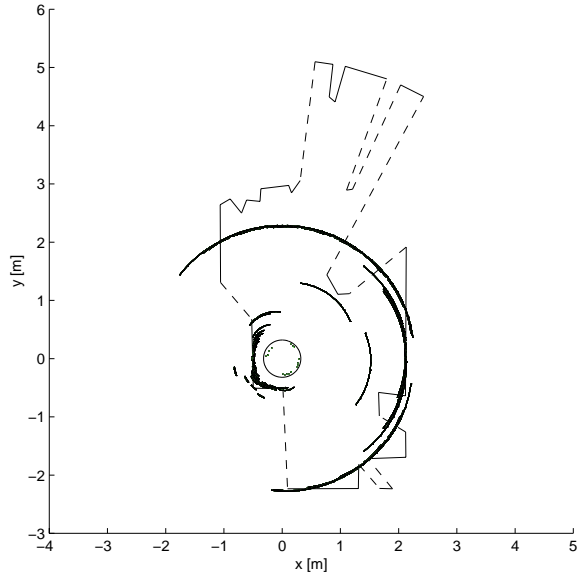


Figure 4: Distance readings from the ultrasonic sensing system

In order to compare actual and simulated distance readings we create two 4-by-24 matrices, one containing the actual echos and the other one containing the simulated echos. The ultrasonic sensing system provides one direct echo and six cross echos for each sensor. The cross echo paths exist two-fold, since both sensors involved are able to transmit and receive ultrasound. Regarding the simulation model, the distance results for both directions are identical. For comparison with the simulated distance readings we reduce the original 7-by-24 matrix obtained from the sensing system to a 4-by-24 matrix. To accomplish this we average over the two-fold existing echo paths and return an error code if the two echos are inconsistent. We also convert the echo path lengths into distance readings, considering the displacement of the involved sensors. Distance readings exceeding the detection range are confined to the maximum value.

Now we subtract the two 4-by-24 matrices and obtain a difference matrix. Then we compare the absolute values of the difference matrix with a distance uncertainty threshold ( $0.1m$ ) and create a so called "simulation-based confidence matrix" with the same dimension. We assign "1" or "0" to the respective element of the simulation-based confidence matrix depending if the difference between an actual and a simulated reading is lower or higher than the threshold. Subsequently we expand the simulation-based confidence matrix to the dimension 7-by-24, which we achieve by adding the redundant echo paths to each column. For each sensor the simulation-based confidence matrix then contains confidence values for one direct echo path and six cross echo paths. We accumulate the confidence values for all sensors by calculating the sum for all columns of the simulation-based confidence matrix and thus obtain a simulation-based confidence vector, which typically looks as follows:

$$\text{simulation\_based\_confidence\_vector} = \{ 7 \ 4 \ 2 \ 2 \ 4 \ 4 \ 4 \ 6 \ 0 \ 1 \ 4 \ 3 \ 3 \ 5 \ 5 \ 3 \ 6 \ 3 \ 5 \ 7 \ 4 \ 4 \ 5 \ 7 \}$$

The elements of the simulation-based confidence vector can adopt values between "0" and "7". If an element value is high, the confidence in this sensor will also be high. If an element value is "0", we will suspect the sensor to be faulty.

## 6 Sensor Evaluation by Calculation of Intersections for the real Ultrasonic Sensor Readings

Within this section we compare the direct and cross

echos obtained from the sensing system among themselves. We assume neighbor echos to be similar, since the sensors are placed close to each other. As already mentioned, the sensing system provides one direct echo and 6 cross echos for each sensor, i. e.  $(1+6)*24 = 168$  echos altogether. Since the detection ranges for various direct and cross echo paths multiple overlap, their distance readings can be compared.

The following echo path overlaps exist for each sensor ( $S_i$ ):

direct echo  $S_i$  with

- direct echos  $S_{i-3}, S_{i-2}, S_{i-1}, S_{i+1}, S_{i+2}, S_{i+3}$
- cross echos  $S_{i-3}/S_{i-2}, S_{i-2}/S_{i-1}, S_{i-1}/S_i,$   
 $S_i/S_{i+1}, S_{i+1}/S_{i+2}, S_{i+2}/S_{i+3}$
- cross echos  $S_{i-3}/S_{i-1}, S_{i-2}/S_i, S_{i-1}/S_{i+1},$   
 $S_i/S_{i+2}, S_{i+1}/S_{i+3}$
- cross echos  $S_{i-3}/S_i, S_{i-2}/S_{i+1}, S_{i-1}/S_{i+2}, S_i/S_{i+3}$

cross echo  $S_i/S_{i-1}$  with

- cross echos  $S_{i-3}/S_{i-2}, S_{i-2}/S_{i-1},$   
 $S_i/S_{i+1}, S_{i+1}/S_{i+2}$
- cross echos  $S_{i-3}/S_{i-1}, S_{i-2}/S_i, S_{i-1}/S_{i+1}, S_i/S_{i+2}$
- cross echos  $S_{i-3}/S_i, S_{i-2}/S_{i+1}, S_{i-1}/S_{i+2}$

cross echo  $S_i/S_{i+1}$  with

- cross echos  $S_{i-2}/S_{i-1}, S_{i-1}/S_i,$   
 $S_{i+1}/S_{i+2}, S_{i+2}/S_{i+3}$
- cross echos  $S_{i-2}/S_i, S_{i-1}/S_{i+1}, S_i/S_{i+2}, S_{i+1}/S_{i+3}$
- cross echos  $S_{i-2}/S_{i+1}, S_{i-1}/S_{i+2}, S_i/S_{i+3}$

cross echo  $S_i/S_{i-2}$  with

- cross echos  $S_{i-3}/S_{i-1}, S_{i-1}/S_{i+1}$
- cross echos  $S_{i-3}/S_i, S_{i-2}/S_{i+1}$

cross echo  $S_i/S_{i+2}$  with

- cross echos  $S_{i-1}/S_{i+1}, S_{i+1}/S_{i+3}$
- cross echos  $S_{i-1}/S_{i+2}, S_i/S_{i+3}$

We notice that 51 overlaps of direct and cross echo paths exist for each sensor. In order to compare the distance readings for these echo paths we calculate the intersections of the circular and elliptic arcs (Figure 5). Here we assume that consistent distance readings intersect within the overlapping range. By calculating intersections for all overlapping echo paths we derive a 51-by-24 "intersection matrix", and assign "1" or "0" to the respective element of this matrix depending whether an intercept point within the overlapping range exists or not exists. We intend to compare distance readings of echo paths were the sensor to be tested is involved with distance readings of overlap-

ping echo paths were this sensor is not involved in order to only consider intersections which are independent from the sensor to be tested. For this reason we remove the respective lines from the intersection matrix and obtain a so called "intersection-based confidence matrix" of dimension 35-by-24. For each sensor the intersection-based confidence matrix then contains confidence values for all possible intersections with echo paths independent from the sensor to be tested. We accumulate the confidence values for all sensors by calculating the sum for all columns of the intersection-based confidence matrix und thus obtain an intersection-based confidence vector, which typically looks as follows:

intersection\_based\_confidence\_vector =  
{ 15 7 2 1 0 1 1 0 1 1 2 3 4 8 8 8 6 4 7 9 6 2 14 13 }

If the value of an element within this vector is high, the confidence in this sensor will also be high. If an element value is "0", we will suspect the sensor to be faulty.

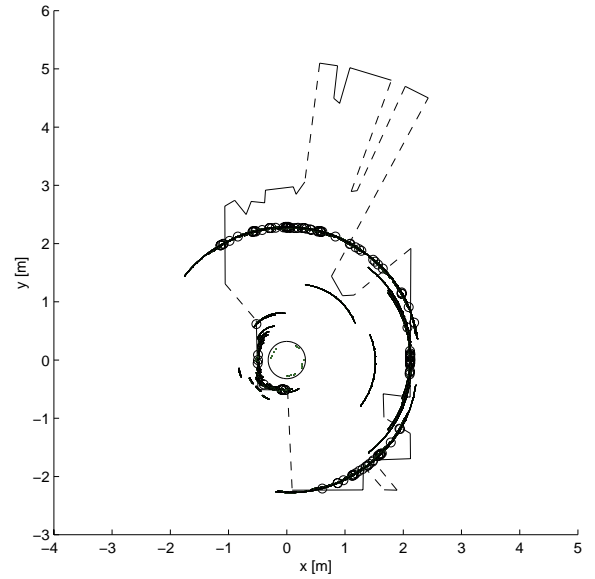


Figure 5: Intersections of circular and elliptic arcs

## 7 Overall Sensor Assessment

In section 5 we compared the actual distance readings obtained from the sensing system to the results obtained with the simulation model, and in section 6 we compared the direct and cross echos obtained from the sensing system among themselves. We can now add the above derived confidence vectors and obtain

a so called "overall confidence vector":

```
overall_confidence_vector =  
simulation_based_confidence_vector +  
intersection_based_confidence_vector =  
{ 22 11 4 3 4 5 5 6 1 2 6 6 7 13 13 11 12 7 12 16 10 6  
19 20 }
```

The overall confidence vector allows us to perform a reliable and robust overall sensor assessment. If an element within this vector becomes "0", we will declare the respective sensor faulty and remove it from the perceptual system. In our example none of the sensors was faulty and none of the overall confidence vector elements is "0".

In order to simulate a fault and to demonstrate the behavior of the error detection system we falsify the distance readings where sensor S<sub>4</sub> was involved and we obtain the following results:

```
simulation_based_confidence_vector =  
{ 6 3 2 0 4 4 4 6 0 1 4 3 3 5 5 3 6 3 5 7 4 4 5 7 }
```

```
intersection_based_confidence_vector =  
{ 12 6 1 0 0 1 1 0 1 1 2 3 4 8 8 8 6 4 7 9 6 2 14 13 }
```

```
overall_confidence_vector =  
{ 18 9 3 0 4 5 5 6 1 2 6 6 7 13 13 11 12 7 12 16 10 6  
19 20 }
```

We can see that `overall_confidence_vector(4)` becomes "0", which indicates a fault on Sensor S<sub>4</sub>.

## 8 Conclusion

We presented a novel error detection method associated with a new ultrasonic sensing system. In this context we described how a two-step approach can provide reliable and robust sensor assessment. In the first step we compared the actual distance readings from the sensing system to results obtained with a simulation model, and in the second step we compared the direct and cross echos from the sensing system among themselves. Based on these two steps we perform an overall sensor assessment. A single ultrasonic scan around the robot will be sufficient to carry out a complete sensor check. Consequently it is not necessary to make observations from different robot positions within the environment, although this would even increase confidence in the assessment results. In ongoing research we undertake error recovery by removing faulty sensors from the perceptual system and navigating with a reduced sensor system.

## Acknowledgment

This work was supported by the German ministry for education, science, research, and technology (BMB+F) under grant no. 01 IL 902 F 6 as part of the project MORPHA.

## References

- [1] D. Bank, M. Strobel, E. Prassler. "AutoBed - An Automatically Guided Hospital Bed". *IASTED International Conference Robotics and Applications RA '99*, Santa Barbara, California, USA, pp. 324-329, 1999.
- [2] J. Borenstein, Y. Koren. "The Vector Field Histogram - Fast Obstacle Avoidance for Mobile Robots". *IEEE Transactions on Robotics and Automation*, Vol. 7, No. 3, pp. 278-288, 1991.
- [3] A. Elfes. "Sonar-Based Real-World Mapping and Navigation". *IEEE Journal of Robotics and Automation*, Vol. RA-3, No. 3, pp. 249-265, 1987.
- [4] J. J. Leonard, H. F. Durrant-Whyte. *Direct Sonar Sensing for Mobile Robot Navigation*, Kluwer Academic Publishers, 1992.
- [5] F. Lu. "Shape Registration using Optimization for Mobile Robot Navigation". *PhD Thesis, University of Toronto*, Toronto, Canada, 1987.
- [6] E. Prassler, D. Bank, J. Illmann, J. Scholz, M. Strobel, P. Fiorini. "An Autonomous Passenger Transportation System for Public, Crowded Environments". *Robotik 2000*, VDI Berichte Nr. 1552, pp. 383-390, Berlin, Germany, 2000.
- [7] M. Soika. "Grid Based Fault Detection and Calibration of Sensors on Mobile Robots". *Proceedings of the IEEE International Conference on Robotics and Automation*, Albuquerque, New Mexico, USA, 1997.
- [8] B. Wirnitzer, W. Grimm, H. Schmidt, R. Klinnert. "Interference Cancelling in Ultrasonic Sensor Arrays by Stochastic Coding and Adaptive Filtering". *IEEE International Conference on Intelligent Vehicles*, Stuttgart, Germany, 1998.